

Optical-model potential in single-nucleon-transfer reactions induced by heavy ions*

W. Henning, Y. Eisen, J. R. Erskine, D. G. Kovar, and B. Zeidman

Argonne National Laboratory, Argonne, Illinois 60439

(Received 3 May 1976)

Elastic scattering angular distributions were measured for $^{48}\text{Ca} + ^{16}\text{O}$ at 56 MeV and for $^{45}\text{Sc} + ^{15}\text{N}$ at 47.53 MeV. Extensive searches and systematic analyses of the optical-model potentials were performed to study ambiguities. Various potential sets that fit elastic scattering were used in distorted-wave Born approximation calculations of single-nucleon transfers. To a high degree the optical potential ambiguities that exist for elastic scattering persist for the transfer predictions. The distorted-wave Born approximation calculations are compared to experimental angular distributions of the single-proton-transfer reactions $^{48}\text{Ca}(^{16}\text{O}, ^{15}\text{N})^{49}\text{Sc}$ and $^{48}\text{Ca}(^{19}\text{F}, ^{18}\text{O})^{49}\text{Sc}$ at 56 MeV and $^{48}\text{Ca}(^{15}\text{N}, ^{14}\text{C})^{49}\text{Sc}$ at 48 MeV. The transfers are well predicted by the distorted-wave Born approximation when there is l matching between the entrance and exit channel dominant partial waves. For cases of l mismatch the calculations do not reproduce the data. This disagreement cannot be removed by changes in the optical potentials, if these are still required to describe elastic scattering. These results suggest the possible presence of reaction processes other than those treated in the conventional distorted-wave Born approximation amplitude.

[NUCLEAR REACTIONS $^{48}\text{Ca}(^{16}\text{O}, ^{16}\text{O})$, $E = 56$ MeV, $^{45}\text{Sc}(^{15}\text{N}, ^{15}\text{N})$, $E = 47.53$ MeV,
 $^{48}\text{Ca}(^{16}\text{O}, ^{15}\text{N})^{49}\text{Sc}$, $^{48}\text{Ca}(^{19}\text{F}, ^{18}\text{O})^{49}\text{Sc}$, $E = 56$ MeV, $^{48}\text{Ca}(^{15}\text{N}, ^{14}\text{C})^{49}\text{Sc}$, $E = 48$ MeV,
 measured $\sigma(\theta)$, optical model, and DWBA analyses.]

I. INTRODUCTION

Considerable effort has been devoted to an understanding of heavy-ion-induced transfer reactions¹⁻¹⁹ through the use of the first-order distorted-wave Born approximation (DWBA).²⁰⁻²³ Such attempts have been successful in cases where both the spectroscopic overlap between the initial and final configurations is large and where the kinematic conditions correspond to a quasielastic reaction, i.e., good matching for the dominant partial waves l , in the entrance and exit channel. However, as more data have been accumulated it has become evident that for many transfer reactions, strengths and angular distributions deviate markedly from their DWBA predictions.^{15,16,24-31} Since a large number of parameters enter such calculations through the entrance and exit channel optical potentials and through the properties of the bound state wave functions, the origin of such failures could be a consequence of an incorrect choice of these parameters. An investigation of this question is clearly necessary before any relevant conclusions regarding basic shortcomings in the DWBA formalism can be drawn. In the present paper we limit ourselves to questions regarding the optical-model parameters. Specifically we investigate the effects of optical-model ambiguities that result from fits to elastic scattering data when these parameter sets are used in the DWBA calculations.

It has been suggested³² that angular distributions of heavy-ion-induced transfer reactions and, in particular, the oscillatory structure at forward

angles might prove useful in determining the average ion-ion potential. This expectation arises from the observation that small changes in the optical-model parameters may introduce large changes in the calculated angular structure of such transfer cross sections while altering the elastic scattering predictions only little. A number of investigations have been performed³³⁻³⁷ which were apparently successful in reducing optical-model ambiguities through transfer data. However, our preliminary studies did not support these findings.³⁸

To study this problem more carefully, we have measured elastic scattering and single-nucleon-transfer reactions. Angular distributions of elastic scattering were measured for $^{48}\text{Ca} + ^{16}\text{O}$ at 56 MeV and $^{45}\text{Sc} + ^{15}\text{N}$ at 47.53 MeV. The second system was chosen to represent the outgoing channel in the ($^{16}\text{O}, ^{15}\text{N}$) reaction on Ca isotopes. Since ^{45}Sc is the only stable Sc isotope usable as a target, the $^{45}\text{Sc} + ^{15}\text{N}$ potential is taken to be representative for the other Sc isotopes. One-proton transfers on ^{48}Ca were measured via the ($^{16}\text{O}, ^{15}\text{N}$), ($^{15}\text{N}, ^{14}\text{C}$), and ($^{19}\text{F}, ^{18}\text{O}$) reactions. The reactions proceed under different kinematic conditions to the same final states in ^{49}Sc . Extensive optical-model and DWBA transfer calculations were performed and compared to the data.

Section II describes the experimental methods used. In Section III the elastic scattering results are discussed and optical-model calculations are presented. Section IV shows the transfer predictions of DWBA calculations employing the optical-model parameters deduced in Sec. III. In Sec. V

the transfer predictions are compared to the data. Section VI summarizes our conclusions.

II. EXPERIMENTAL METHOD AND RESULTS

The measurements were performed with two different experimental setups: (a) a split-pole magnetic spectrograph with a position sensitive resistive wire proportional counter at the focal plane,³⁹ and (b) a ΔE - E surface barrier detector, time-of-flight telescope.⁴⁰ The focal plane proportional counter yielded a ΔE signal of about 5% resolution which together with the high momentum resolution of the spectrograph was sufficient to separate the strongest particle groups. The energy resolution was typically of the order of 80–170 keV and mainly determined by the finite target thickness. The time-of-flight system guaranteed complete channel resolution for all transfer channels but the energy resolution was typically 250 keV.

The $^{48}\text{Ca}(^{16}\text{O}, ^{15}\text{N})^{49}\text{Sc}$ reaction was measured independently with both systems and yielded consistent results for resolved states. The $^{48}\text{Ca}(^{15}\text{N}, ^{14}\text{C})^{49}\text{Sc}$ reaction was measured with the split-pole spectrograph and the $(^{19}\text{F}, ^{18}\text{O})$ reaction with the time-of-flight telescope. In addition some data points for the $(^{19}\text{F}, ^{18}\text{O})$ reactions and the optical-model parameters for $^{48}\text{Ca} + ^{19}\text{F}$ elastic scattering were taken from Ref. 41. The $^{48}\text{Ca} + ^{16}\text{O}$ elastic scattering reaction was also measured with both systems; the $^{45}\text{Sc} + ^{15}\text{N}$ reaction with the spectrograph. An absolute normalization was obtained from elastic scattering measurements at forward angles. Relative normalizations were obtained through the use of a fixed monitor counter and the integrated particle current in the Faraday cup. The electronic system eliminated pileup and provided an exact measure of the deadtime.⁴⁰ For the time-of-flight system small angle scattering losses were measured and found to vary monotonically over the angular range with a maximum of 15%. With this correction applied the spectrograph and time-of-flight data agreed. Because of the large dynamic range of the split-pole magnetic spectrograph, the 50 cm long focal plane detector simultaneously recorded the two dominant charge states of the outgoing ions ($^{16}\text{O}^{8+,7+}$, $^{15}\text{N}^{7+,6+}$, and $^{14}\text{C}^{6+,5+}$). At regular intervals, the $^{16}\text{O}^{8+}$, $^{15}\text{N}^{5+}$, and $^{14}\text{C}^{4+}$ charge states, which account for less than 3% of the total yield, were also measured. The error introduced through the neglect of the smaller charge states is estimated to be less than 0.5% of the total yield. Figure 1 shows energy spectra for two of the single-proton-transfer reactions measured. The angular distributions for elastic scattering and transfer reactions will be discussed in the following sections.

III. ELASTIC SCATTERING AND OPTICAL-MODEL ANALYSIS

Before discussing the details of the optical-model analysis we reiterate that the main emphasis in the elastic scattering study is not to obtain general information about the ion-ion potential, but rather to study the implications of the optical potential on the DWBA analysis of transfer reactions. Although both are interrelated and cannot be considered totally independently, our effort is primarily directed toward the second aspect.

The $^{48}\text{Ca} + ^{16}\text{O}$ elastic scattering angular distribution at 56 MeV bombarding energy is shown in Fig. 2. The ratio for elastic scattering to Rutherford scattering, σ/σ_R , has been measured to a lower value of about 3×10^{-3} . Optical-model fits performed with the codes ABACUS⁴² and GENOA⁴³ yielded identical results after a careful choice of integration step sizes and the cutoff radius. Calculations with ABACUS were found to be more sensitive to the integration parameters and care had to be taken to prevent spurious oscillations in the calculated cross sections. Optical-model fits were performed with various types of starting potentials taken from the literature.^{32,35,44-49} All of these have been considered typical for heavy-ion scattering in the mass and energy range being studied and some have been touted as the most appropriate ones. The potential was of a Wood-Saxon type. Six parameters were varied independently: depths (V, W), radii (r_{or}, r_{oi}), and diffusenesses (a_r, a_i) for real and imaginary parts of the potential. The decision to vary six parameters was made in order to obtain rather equivalent elastic scattering predictions, since the main purpose of this study is to investigate whether the additional information extracted from the transfer reactions resolves ambiguities in parameters that exist in the analysis of the elastic scattering.

Potentials that fit the elastic scattering for the $^{48}\text{Ca} + ^{16}\text{O}$ system at 56 MeV incident energy are listed as potentials A in Table I. First we find that the typical features of the original starting potentials are maintained and the parameters are only moderately altered; this is also true for the potentials that were originally of the four-parameter type. Secondly, we observe that extending data from $\sigma/\sigma_R \approx 10^{-2}$ to $\approx 10^{-3}$ does not remove potential ambiguities; the calculations yield small changes in the various parameter sets and differ only in the region not constrained by data. However, in view of the possible complexity of the reaction processes discussed later, the extension of optical-model fits to elastic scattering data many orders of magnitude below Rutherford scattering appears *ab initio* questionable. Finally, the

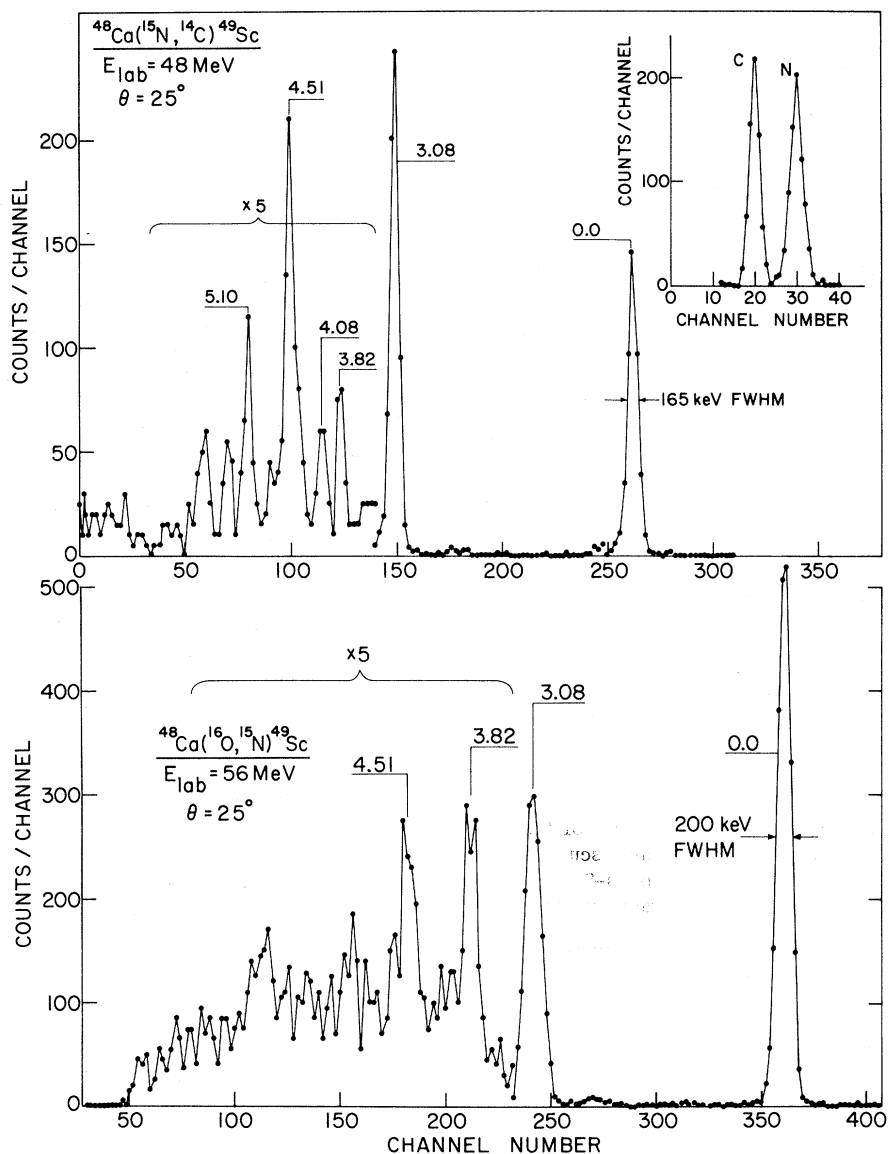


FIG. 1. Energy spectra of the single-proton-transfer reactions ($^{15}\text{N}, ^{14}\text{C}$) and ($^{16}\text{O}, ^{15}\text{N}$) on ^{48}Ca leading to various states in ^{49}Sc .

quality of the fits is nearly equal with respect to χ^2 (Table II, last column); the relative deviations from the average value $\chi^2 = 1.7$ is about $\pm 25\%$. The absolute value is only of limited significance, since the errors were chosen as statistical errors when larger than 1%, but kept at a systematic limit of 1% when the statistical error was smaller.

Before studying the detailed features of these potentials let us consider the results for the elastic scattering for $^{45}\text{Sc} + ^{15}\text{N}$. They were treated in an identical fashion as the $^{48}\text{Ca} + ^{16}\text{O}$ data. Figure 3 shows the experimental angular distribution and the optical-model fits. The optical-model param-

eters are listed in Table I as Set B. In addition to the same features as found for the $^{48}\text{Ca} + ^{16}\text{O}$ system we find a large similarity between Sets A and B. Within the limits determined by the accuracy of our data, they are identical. We cannot conclude from this similarity that there is a general ion-ion potential for collisions in heavy-ion systems of masses as the ones studied here. It has been shown,⁵⁰ for example, that ^{18}O and ^{16}O elastic scattering yield quite different potentials because of the stronger absorption in the ^{18}O systems which is attributed to its strong inelastic excitations. It appears, however, that ions without

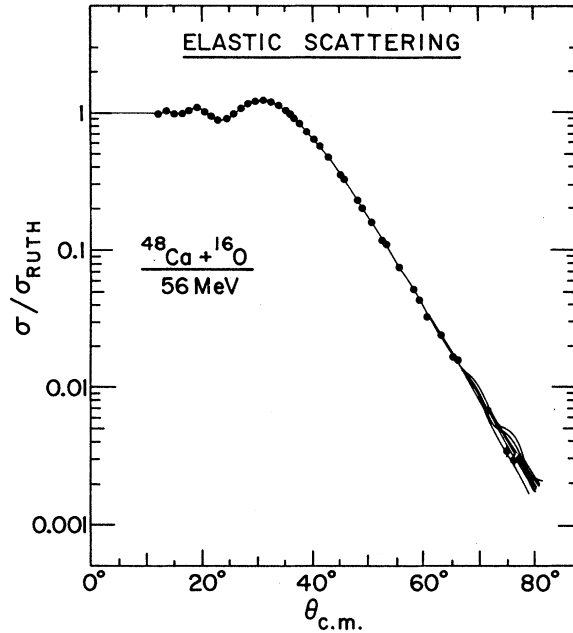


FIG. 2. Elastic scattering angular distributions for $^{48}\text{Ca} + ^{16}\text{O}$ at 56 MeV. The solid lines are various optical-model fits as discussed in the text.

TABLE I. Optical potential parameter sets for the systems $^{48}\text{Ca} + ^{16}\text{O}$ (A) and $^{45}\text{Sc} + ^{15}\text{N}$ (B) as discussed in the text. The optical potential $V(r)$ of Woods-Saxon shape is given in terms of the listed parameters by the following expressions:

$$V(r) = -V_0 [f(r, R_r, a_r) - iW_0 \\ \times [f(r, R_i, a_i)], \\ R_r = r_{or} (A_1^{1/3} + A_2^{1/3}), \\ R_i = r_{oi} (A_1^{1/3} + A_2^{1/3}), \\ f(r, R, a) = [1 + \exp[(r - R)/a]]^{-1}.$$

Potential	V_0	r_{or}	a_r	W_0	r_{oi}	a_i
A1	313	1.208	0.408	105	1.337	0.188
B1	319	1.205	0.408	92	1.326	0.176
A2	149	1.168	0.496	11.1	1.233	0.566
B2	150	1.170	0.507	10.8	1.211	0.541
A3	100	1.200	0.500	24.0	1.207	0.482
B3	108	1.202	0.504	26.9	1.185	0.481
A4	78	1.218	0.497	11.3	1.232	0.571
B4	82	1.221	0.502	9.3	1.216	0.553
A5	43.5	1.259	0.520	48.0	1.203	0.458
B5	45.0	1.262	0.525	42.3	1.194	0.452
A6	33.8	1.344	0.424	110.2	1.274	0.280
B6	35.9	1.349	0.425	96.7	1.272	0.275
A7	12.7	1.363	0.510	8.0	1.363	0.510
B7	13.3	1.367	0.522	6.7	1.349	0.488

TABLE II. Various quantities as deduced from the optical-model parameters Sets A of Table I for the system $^{48}\text{Ca} + ^{16}\text{O}$.

Potential	$l_{1/2}$	$R_{1/2}$	$V(R_{1/2})$ (MeV)	$W(R_{1/2})$ (MeV)	σ_r (b)	χ^2
A1	30.36	9.43	-2.3	-0.17	1.281	1.4
A2	30.21	9.44	-1.6	-0.40	1.313	1.5
A3	30.18	9.44	-1.6	-0.37	1.290	1.7
A4	30.16	9.44	-1.5	-0.42	1.313	1.4
A5	30.15	9.43	-1.7	-0.57	1.306	1.3
A6	30.30	9.43	-2.1	-0.37	1.286	1.5
A7	29.86	9.38	-1.6	-1.00	1.303	2.1

strong low-energy excitations as ^{16}O , ^{15}N , and presumably ^{14}C have a quite similar average interaction with targets of the mass region studied here. We note this because, in general, for studies of heavy-ion transfer reactions elastic scattering data for the outgoing channels are not readily obtained inasmuch as the outgoing projectiles or final target nuclei are often unstable or hard to produce.

Let us consider the common feature of the potentials listed in Table I. Because of the surface nature of the heavy-ion elastic scattering at the energies studied here, we expect large similarities in the surface part of the potentials and in physical quantities associated with it, as in Blair's discussion of elastic α scattering.⁵¹ The real (V) and imaginary potentials (W) as a function of relative radial coordinate r between the two ions are shown in Figs. 4 and 5. The real potentials, despite their

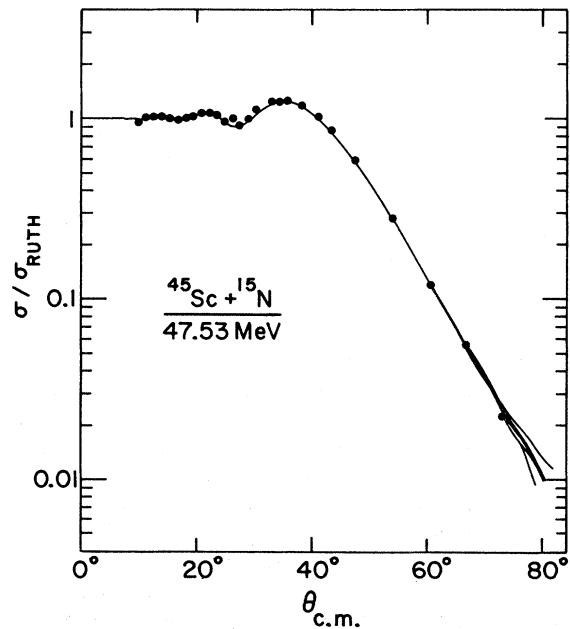


FIG. 3. Elastic scattering angular distribution for $^{45}\text{Sc} + ^{15}\text{N}$ at 47.53 MeV.

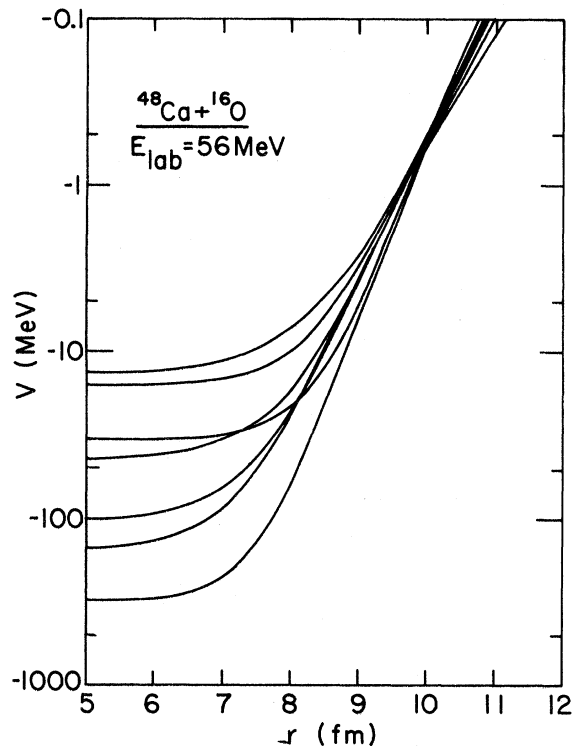


FIG. 4. Shape of the real part $V(r)$ of the optical potential for the elastic scattering of $^{48}\text{Ca} + ^{16}\text{O}$ for various potential parameter sets.

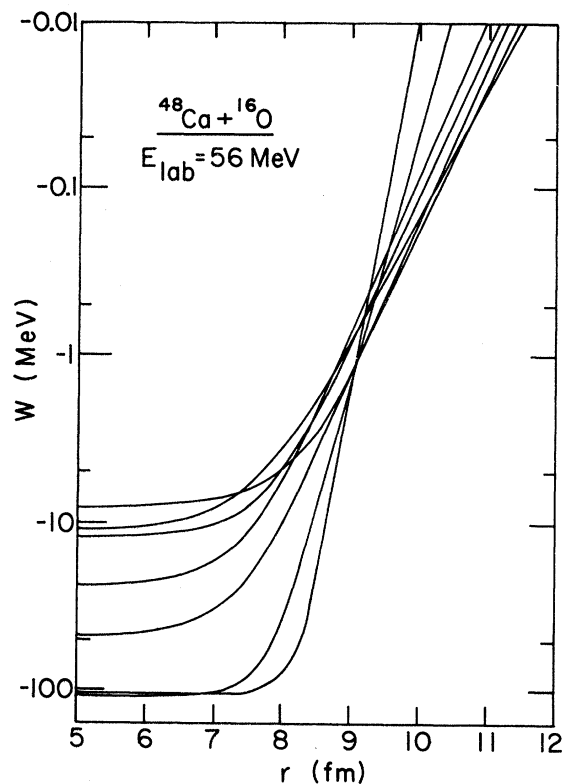


FIG. 5. Shape of the imaginary part $W(r)$ of the optical potential for the elastic scattering of $^{48}\text{Ca} + ^{16}\text{O}$ for various potential parameter sets.

very large differences in depths in the nuclear interior, approach a nearly constant value at approximately $r=10$ fm and have close values over the range $9 \text{ fm} \leq r \leq 10 \text{ fm}$. However, because of their different slopes in the asymptotic tail region, they do not represent potential ambiguities of the type described by Igo.⁵² No such close values exist for the imaginary potentials, although for a small region around 9 fm all values lie within a factor of 2.5. It appears that the imaginary potential is required to be sufficiently large in the interior so as to absorb all flux for close collisions. This is demonstrated by the transmission coefficients for the various potentials as shown in Fig. 6. All partial waves below $l=26$ are totally absorbed and this results in partial wave reaction cross sections equal to the unitarity limit, as shown in Fig. 7. The hatched band in this figure indicates the range of values obtained by employing the various optical potential sets.

From the transmission coefficients or the scattering amplitudes we can now deduce a half value $l_{1/2}$ corresponding to an average surface partial wave l value. Following Blair,⁵¹ we take the l value where the real part of the scattering S matrix goes

through 0.5 and deduce the value of $l_{1/2}$ given in Table II. From the total energy relation

$$E = V_n + \frac{Z_1 Z_2 e^2}{R_{1/2}} + \frac{\hbar^2}{2\mu} \frac{l_{1/2}(l_{1/2} + 1)}{R_{1/2}^2},$$

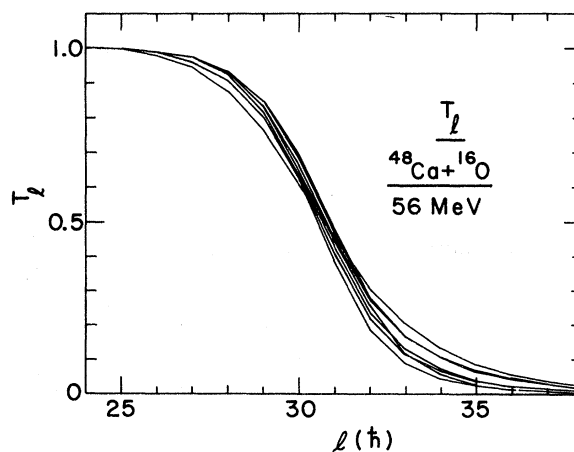


FIG. 6. Transmission coefficients T_l as a function of partial wave angular momentum l for various optical potential parameter sets as given in Table I.

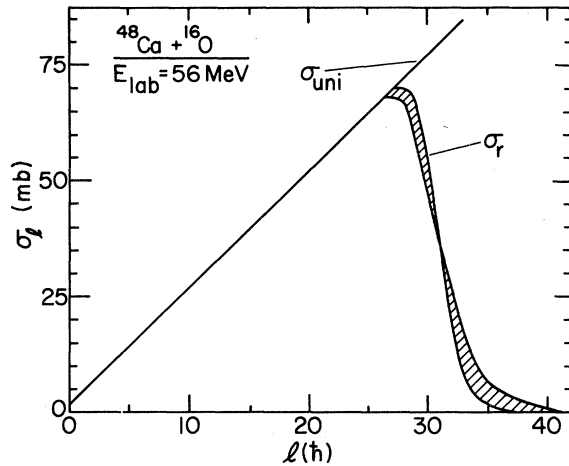


FIG. 7. Partial wave reaction cross section σ_l for $^{48}\text{Ca} + ^{16}\text{O}$ at 56 MeV. The hatched area indicates the range of σ_l for the various optical potential parameter sets given in Table I.

we then iteratively deduce a half radius $R_{1/2}$ which is also listed in Table II. Here V_n is the nuclear potential, μ the reduced mass, and Z_1, Z_2 the nuclear charge of the projectile and target, respectively. We find that $l_{1/2}$ and, as a consequence, $R_{1/2}$ are highly constant for all potential sets. As one would expect from Figs. 6 and 7, this is also true for the total reaction cross sections, listed in Table II. Also listed are the values of real and imaginary potentials at $r=R_{1/2}$. As observed before, $V(R_{1/2})$ is nearly constant to within about $\pm 30\%$ from the average value, whereas $W(R_{1/2})$ varies as much as a factor of 6 at this particular radius. In conclusion, we find that the ambiguities in the elastic scattering distribution and the deduced quantities arise mainly from two features of the potentials considered: (a) the complete absorption in the interior for $l \leq 26$, even for the "weakest absorbing" potential, and (b) nearly constant strengths of the real potentials at the nuclear surface in the vicinity of the strong absorption radius $R_{1/2}$.

Inspection of the complex scattering amplitudes for the surface partial waves $l=25$ to 35 shows that the amplitudes from different parameter sets are to a very large extent equivalent. This is obviously a result of the delicate interplay between real and imaginary potentials and their effect on phases and amplitudes, superimposed upon the gross features discussed above. The choice of six parameters facilitates the generation of equivalent amplitudes. For the dominant partial waves the radial wave functions are also nearly identical at the nuclear surface. We emphasize this point because, if transfer reactions yield additional

information concerning the average potential, they must be sensitive to different partial waves and a different nuclear region.

IV. DWBA PREDICTIONS FOR TRANSFER PROCESSES

Since additional complexities arise in DWBA calculations if more than one particle is transferred, we restrict our investigation to single-proton transfers. This has the additional advantage that spectroscopic factors are generally known from light-ion-induced reactions, such as ($^3\text{He}, d$), and can be used as additional checks on heavy-ion-induced transfer reactions.

The DWBA calculations were performed using the exact finite-range code LOLA in the post representation. In all calculations the conventional separation energy prescription with Woods-Saxon parameter $r_0=1.25$ fm and $a_0=0.65$ fm was used to generate the bound state wave functions for both target and projectile. Spin-orbit terms were neglected. The transfer interaction in all cases was taken to include only the nuclear part.⁵³

The optical-model parameter sets of Sec. III which are found to produce equivalent fits to the elastic scattering of $^{16}\text{O} + ^{48}\text{Ca}$ are used to calculate DWBA predictions for the one-proton-transfer reactions $^{48}\text{Ca}(^{16}\text{O}, ^{15}\text{N})^{49}\text{Sc}$ leading to the $f_{7/2}$ ground state and the $p_{3/2}$ first excited state at 3.08 MeV in ^{49}Sc . The results are shown in Fig. 8. Although there are small differences in shape, the DWBA predictions are practically equivalent for both states. The curves have been arbitrarily normalized so as to produce maximum overlap; however, the relative normalization differs by no more than $\pm 15\%$. The same potential has been used for both the ingoing and outgoing elastic channels in view of the close agreement between Sets A and B in Table I. This is further justified through transfer calculations for the $^{48}\text{Ca}(^{16}\text{O}, ^{15}\text{N})^{49}\text{Sc}$ reaction using each of two parameter sets (A3 and B3) in both entrance and exit channel, and using A3 in the entrance and B3 in the exit channel and vice versa. The results overlap well with the band of curves in Fig. 8. As a further example, DWBA predictions for a different reaction, namely $^{48}\text{Ca}(^{15}\text{N}, ^{14}\text{C})^{49}\text{Sc}(\text{g.s.})$ at 48 MeV are shown in Fig. 9 for the various potential sets.

From the DWBA calculations we conclude that the close agreement between predictions for different potentials indicates that the same partial waves dominate the angular distributions for both the transfer and elastic scattering.⁵⁴ This is valid for reactions where the ingoing and outgoing dominant partial waves overlap well within the range spanned by the transferred angular momentum ("well matched" or "quasielastic") such as the

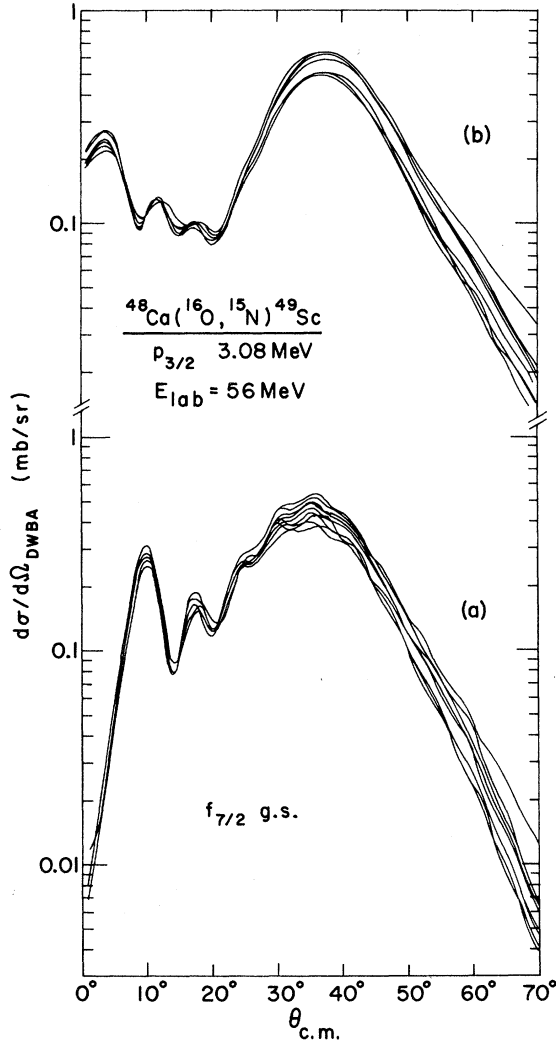


FIG. 8. (a) DWBA transfer predictions with code LOLA (Ref. 13) for the $^{48}\text{Ca}(^{16}\text{O}, ^{15}\text{N})^{49}\text{Sc}(f_{7/2}, \text{g.s.})$ reaction; (b) for the $^{48}\text{Ca}(^{16}\text{O}, ^{15}\text{N})^{49}\text{Sc}(p_{3/2}, 3.08 \text{ MeV})$ reaction at 56 MeV.

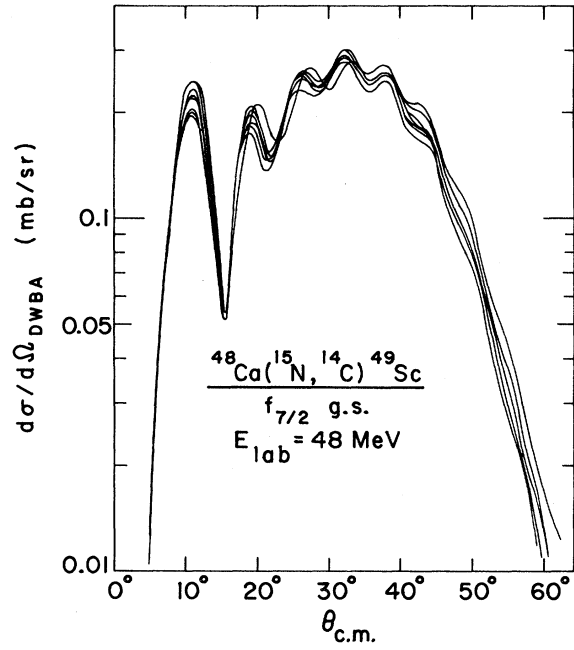


FIG. 9. DWBA transfer prediction for $^{48}\text{Ca}(^{15}\text{N}, ^{14}\text{C})^{49}\text{Sc}(f_{7/2}, \text{g.s.})$.

transfer to the $f_{7/2}$ state in the $^{48}\text{Ca}(^{16}\text{O}, ^{15}\text{N})^{49}\text{Sc}$ reaction. However, this also holds for the “mismatched” transfer to the $p_{3/2}$ state; the matching condition can be read from the $l_{1/2}$ values listed in Table III. In the latter case this might appear surprising since it is found in DWBA calculations of mismatched light-ion-induced reactions that the nuclear interior contributes considerably. However, in heavy-ion collisions the total flux penetrating the nuclear interior is absorbed (Figs. 6 and 7).

Some caution, however, should be exercised with respect to the generality of the argument that the same partial waves dominate elastic scattering and

TABLE III. Ingoing and outgoing channel dominant partial waves l_{in} and l_{out} as discussed in the text. L is the transferred (no-recoil) angular momentum, $a_r^{\text{out}*}$ the modified real diffuseness (if different from a_r^{in}) in the outgoing channel optical potential.

Reaction	State	l_{in}	l_{out}		a_r^{in}	$a_r^{\text{out}*}$	L
			$(a_r^{\text{out}} = a_r^{\text{in}})$	$(a_r^{\text{out}*} \geq a_r^{\text{in}})$			
$(^{15}\text{N}, ^{14}\text{C})$	$f_{7/2}$	27.6	28.3	29.7	0.50	0.60	4
	$p_{3/2}$	27.6	25.5	27.4	0.50	0.60	2
$(^{16}\text{O}, ^{15}\text{N})$	$f_{7/2}$	30.5	29.4	29.4	0.50	0.50	4
	$p_{3/2}$	30.5	26.9	28.4	0.50	0.58	2
$(^{19}\text{F}, ^{18}\text{O})$	$f_{7/2}$	31.2	34.1	38.5	0.50	0.75	3
	$p_{3/2}$	31.2	30.8	30.8	0.50	0.50	1

transfer reactions in a given ion-ion scattering situation. In a transfer reaction the form factor plays a dominant role in determining the distance that contributes most to the transfer cross section. Because of the high correspondence between coordinate and l space in a heavy-ion reaction, the partial wave contribution will depend on the form factor. In multinucleon transfers for example the form factor is expected to fall more steeply and possibly enhance smaller l values, or a smaller band of l values.

We can summarize the results of the DWBA predictions for a given ion-ion system in the mass region studied as follows: When optical-model parameters that give equivalent fits to elastic scattering are used in DWBA calculations similar single-nucleon-transfer predictions result. This is independent of the l matching between incoming and outgoing elastic channels.

V. COMPARISON OF DWBA PREDICTIONS AND TRANSFER DATA

Comparisons of the DWBA predictions for the $^{48}\text{Ca}(^{16}\text{O}, ^{15}\text{N})^{49}\text{Sc}$ reaction leading to the $f_{7/2}$ ground state and first excited $p_{3/2}$ state at 3.08 MeV with

experimental angular distributions are shown in Fig. 10. The solid lines are calculated using the optical parameter Set B3. The $f_{7/2}$ ground state transition is rather well described while the angular distribution for the transfer to the $p_{3/2}$ state is mispredicted. From the results of Sec. IV it is seen that all other optical-model sets will equally mispredict the $p_{3/2}$ state angular distribution. However, as seen in Table III the well-predicted $f_{7/2}$ transition corresponds to a well l -matched situation while the $p_{3/2}$ transition does not.

In order to further investigate the effect of l matching we have measured the $(^{15}\text{N}, ^{14}\text{C})$ and the $(^{19}\text{F}, ^{18}\text{O})$ one-proton transfer reactions on ^{48}Ca which lead to the same $f_{7/2}$ and $p_{3/2}$ states. Because of the different Q values and charges in the incoming and outgoing channels the kinematic conditions differ. While the $(^{16}\text{O}, ^{15}\text{N})$ reaction is well matched for the $f_{7/2}$ ground state, the $(^{19}\text{F}, ^{18}\text{O})$ reaction is well matched for the $p_{3/2}$ excited state; l matching occurs for the $(^{15}\text{N}, ^{14}\text{C})$ reaction half way between both states (see Table III).

If we now compare DWBA predictions and data for the three reactions shown in Fig. 10, we find that in cases of l matching, the data are well predicted by the DWBA calculations. In cases of mis-

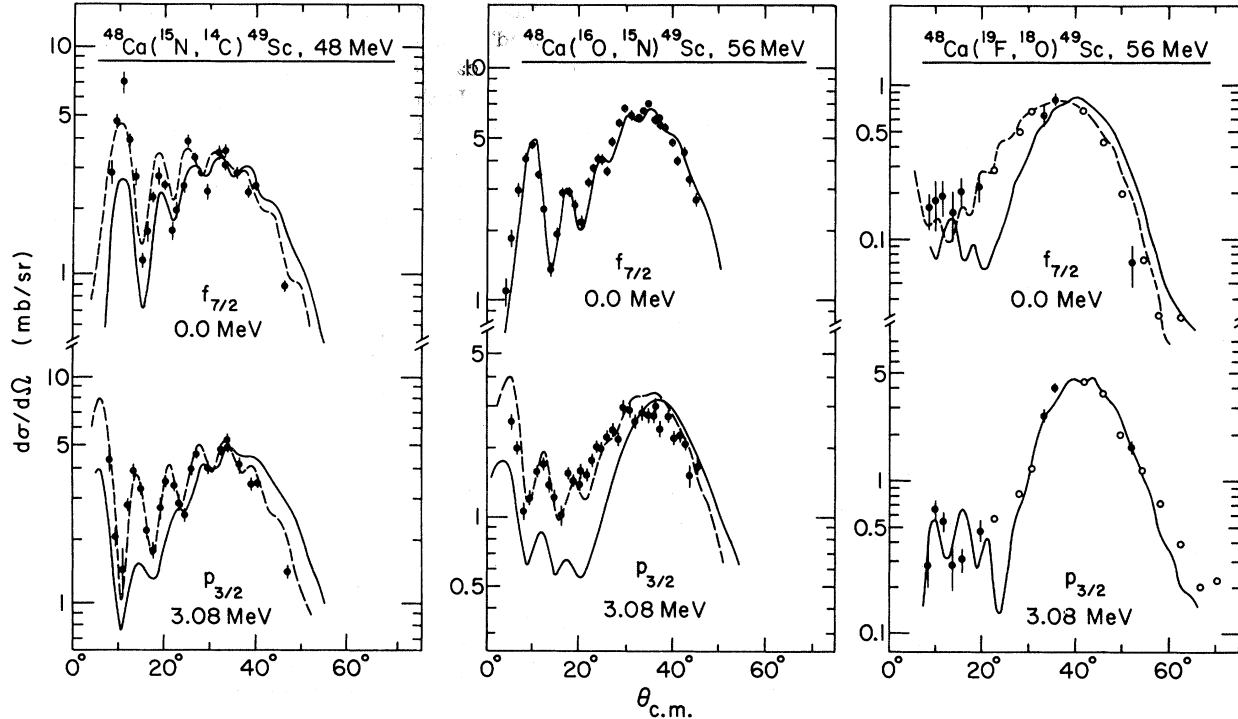


FIG. 10. Angular distributions for the single-proton-transfer reactions $(^{15}\text{N}, ^{14}\text{C})$, $(^{16}\text{O}, ^{15}\text{N})$, and $(^{19}\text{F}, ^{18}\text{O})$ leading to the $f_{7/2}$ ground state and 3.08 MeV excited state in ^{49}Sc . The solid curves are DWBA predictions, calculated with optical-model parameters that fit elastic scattering and with bound state wave functions that are generated by fitting the binding energy in a real Woods-Saxon potential with fixed radius $R = 1.25 \text{ fm} \times A^{1/3}$ and diffuseness $a = 0.65 \text{ fm}$. The dashed curves are calculated with modified optical-model parameters as discussed in the text.

match, discrepancies exist between data and predictions. The degree of discrepancy appears to be related to the degree of mismatch, and the transferred angular momentum L . The difference $l_{in} - l_{out}$ is largest for the $p_{3/2}$ state populated in the ($^{16}\text{O}, ^{15}\text{N}$) reaction, and for the $f_{7/2}$ state populated in the ($^{19}\text{F}, ^{18}\text{O}$) reaction. While both are badly fit, the discrepancy appears to be larger for the $p_{3/2}$ state which is populated via primarily $L = 2$ than for the $f_{7/2}$ state populated by $L = 3$. For the ($^{15}\text{N}, ^{14}\text{C}$) reaction the Q value for $l_{in} - l_{out}$ lies midway between the $f_{7/2}$ and $p_{3/2}$ states. Again both are mispredicted by the DWBA, but the discrepancy for the $f_{7/2}$ state, populated mainly by $L = 4$, is less serious than that observed for the $p_{3/2}$ state, populated mainly by $L = 2$.

There are optical potentials which do not fit elastic scattering but do provide fits to the transfer data even for the mismatched cases. However, these results may be of limited significance since different reaction mechanisms may contribute and the adjusted optical parameters may mask these effects rather than lead to their understanding. It is found that for the ($^{16}\text{O}, ^{15}\text{N}$) reaction leading to the $p_{3/2}$ final state in ^{49}Sc , the disagreement between DWBA and data is easily reduced by an increase in real diffuseness a_r in the outgoing channel (dashed curve in Fig. 10). Such improvement between DWBA predictions and data through an increase in the diffuseness of the outgoing channel optical potential has been noted previously.⁵⁵ An inspection of the elastic scattering amplitudes reveals the effect of this change in diffuseness. As seen in Table III, the dominant partial waves in the outgoing channel are shifted to higher l values. This shift of the transition amplitude increases the overlap between the incoming and outgoing elastic channel. In other words, for a mismatched case the reaction mechanism appears to proceed mainly through the dominant partial wave region of the incoming channel, to a larger extent than predicted by the conventional DWBA. However, this explanation can only explain part of the data.

For the $^{48}\text{Ca}(^{15}\text{N}, ^{14}\text{C})^{49}\text{Sc}$ reaction where a matched situation corresponds to a Q value half way between the $f_{7/2}$ ground state and $p_{3/2}$ excited state, we find that agreement between DWBA and data is obtained for both states if, in both cases, the diffuseness in the outgoing optical potential is increased. For the $p_{3/2}$ final state this means increased overlap between the dominant partial waves in the incoming and outgoing channels, but for the $f_{7/2}$ ground state, this results in an even larger shift between them. This is substantiated by the $^{48}\text{Ca}(^{19}\text{F}, ^{18}\text{O})^{49}\text{Sc}$ reaction where the $p_{3/2}$ excited state is matched and well described by DWBA. However, the $f_{7/2}$ ground state mismatch is in-

creased when the real diffuseness in the outgoing optical potential is increased, even though the DWBA predictions are in agreement with the data (dashed curve Fig. 10).

An additional feature that emerges with these improved DWBA predictions is that the spectroscopic factors deduced agree fairly well with those from light-ion data⁵⁶ (Table IV). This might appear to be of significance, since the forward angle predictions between the original and the changed potential can differ by factors of 5. However, both predictions agree closely in the region of the grazing bump where most of the cross section originates. It appears that some back angle cross section strength is moved to forward angles. This suggests the presence of additional coherent processes such as two-step or multistep processes whose treatment has to await future detailed calculations.

VI. CONCLUSIONS

The purpose of the present investigation was to study the sensitivity to the optical potential in single-nucleon-transfer reactions induced by heavy ions. Since our study is limited to masses around $A = 48$ and bombarding energies about twice the energy of the Coulomb barrier we cannot draw general conclusions with respect to all heavy-ion-induced transfer reactions. The systematics of our calculations and data, however, point to some features which are expected to be valid for a wider range of heavy-ion-induced transfers.

We find that at a given energy the optical potential parameter ambiguities for elastic scattering persist in DWBA predictions for single-nucleon-transfer reactions in the same system. Thus, discrepancies between DWBA predictions and data cannot be removed by a different optical parameter set, if the latter is still required to reproduce the elastic scattering. The experimental angular distributions are well reproduced by standard DWBA predictions only for cases of good l matching. For cases of l mismatch, discrepancies arise which seem to indicate the effects of coherent reac-

TABLE IV. Spectroscopic factors as deduced from the various single-proton-transfer reactions leading to the $f_{7/2}$ ground state and first excited $p_{3/2}$ state at 3.08 MeV in ^{49}Sc . The last row gives the ground state Q values of the reactions.

State	($^3\text{He}, d$) ^a	($^{15}\text{N}, ^{14}\text{C}$) ^b	($^{16}\text{O}, ^{15}\text{N}$) ^b	($^{19}\text{F}, ^{18}\text{O}$) ^b
$f_{7/2}$	1.0	1.68	1.04	1.8
$p_{3/2}$	0.68	0.87	0.56	0.45
Q (MeV)	+4.125	-0.588	-2.504	+1.626

^a Reference 56.

^b This work.

tion processes other than the conventional one-step DWBA amplitude. If one departs from the original DWBA prescription requiring the use of elastic scattering distorted waves, one can find adjusted optical potentials which do reproduce transfer angular distributions under mismatch conditions. These result in a shift of the outgoing dominant partial waves to higher l values, independent of the increased or decreased overlap with the entrance channel partial waves. The significance of these changes is not clear and may in fact simulate additional reaction processes. Further systematic

studies and attempts to understand the reaction mechanisms are underway.

ACKNOWLEDGMENTS

We would like to thank Dr. M. H. Macfarlane, Dr. J. P. Schiffer, Dr. D. A. Goldberg, and Dr. J. G. Cramer for their discussions and comments. We also would like to thank Dr. J. Yntema for his support in taking some of the ^{19}F -induced transfer data.

*Work performed under the auspices of the U. S. Energy Research and Development Administration.

- ¹R. M. Drisko, G. R. Satchler, and R. H. Bassel, in *Proceedings of the Third International Conference on Reactions between Complex Nuclei, Asilomar, 1963*, edited by A. Ghiorso, R. M. Diamond, and H. E. Conzett (Univ. of California Press, Berkeley, 1963), p. 85; T. Kammuri and R. Nakasima, *ibid.*, p. 163.
- ²P. J. A. Buttle and L. J. B. Goldfarb, Nucl. Phys. **78**, 409 (1966); **A115**, 461 (1968); **A176**, 299 (1971).
- ³T. Sawaguri and W. Tobocman, J. Math. Phys. **8**, 2223 (1967).
- ⁴T. Kammuri and H. Yoshida, Nucl. Phys. **A129**, 625 (1969).
- ⁵F. Schmittroth, W. Tobocman, and A. A. Golestaneh, Phys. Rev. C **1**, 377 (1970).
- ⁶A. J. Baltz and S. Kahana, Phys. Rev. Lett. **29**, 1267 (1972).
- ⁷R. Bock and H. Yoshida, Nucl. Phys. **A189**, 177 (1972).
- ⁸P. Bonche and B. Giraud, Phys. Rev. Lett. **28**, 1720 (1972); Nucl. Phys. **A199**, 160 (1973).
- ⁹M. A. Nagarajan, Nucl. Phys. **A196**, 34 (1972).
- ¹⁰R. J. Ascutto and N. K. Glendenning, Phys. Lett. **45B**, 85 (1973).
- ¹¹L. A. Charlton, Phys. Rev. C **8**, 146 (1973).
- ¹²R. M. DeVries and K. I. Kubo, Phys. Rev. Lett. **30**, 325 (1973).
- ¹³R. M. DeVries, Phys. Rev. C **8**, 951 (1973).
- ¹⁴C. A. McMahan and W. Tobocman, Nucl. Phys. **A212**, 465 (1973).
- ¹⁵T. Tamura and K. S. Low, Phys. Rev. Lett. **31**, 1356 (1973); K. S. Low and T. Tamura, Phys. Rev. C **11**, 789 (1975).
- ¹⁶B. F. Bayman, Phys. Rev. Lett. **32**, 71 (1974).
- ¹⁷P. Braun-Munzinger and H. L. Harney, Nucl. Phys. **A223**, 381 (1974).
- ¹⁸R. C. Fuller and O. Dragun, Phys. Rev. Lett. **32**, 617 (1974).
- ¹⁹W. A. Friedman, K. W. McVoy, and G. W. T. Shuy, Phys. Rev. Lett. **33**, 308 (1974).
- ²⁰W. Tobocman, *Theory of Direct Nuclear Reactions* (Oxford U.P., London, 1961).
- ²¹N. Austern, R. M. Drisko, E. C. Halbert, and G. R. Satchler, Phys. Rev. **133**, B3 (1964).
- ²²G. R. Satchler, Nucl. Phys. **55**, 1 (1964).
- ²³N. Austern, *Direct Nuclear Reaction Theories* (Wiley, New York, 1970).

- ²⁴P. Bonche, in *Proceedings of the Symposium on Heavy-Ion Transfer Reactions, Argonne, 1973* [ANL Physics Division Informal Report No. PHY-1973B, 1973 (unpublished)], Vol. I, p. 235.
- ²⁵J. B. Ball, O. Hansen, J. S. Larsen, D. Sinclair, and F. Videbaek, Phys. Lett. **49B**, 348 (1974).
- ²⁶S. Kahana, in *Proceedings of the International Conference on Reactions between Complex Nuclei*, edited by R. L. Robinson, F. K. McGowan, J. B. Ball, and J. H. Hamilton (North-Holland, Amsterdam, 1974), p. 189; D. G. Kovar, *ibid.*, p. 235.
- ²⁷R. M. DeVries, M. S. Zisman, J. G. Cramer, K.-L. Liu, F. D. Becchetti, B. G. Harvey, H. Homeyer, D. G. Kovar, J. Mahoney, and W. von Oertzen, Phys. Rev. Lett. **32**, 680 (1974).
- ²⁸J. L. C. Ford, Jr., K. S. Toth, G. R. Satchler, D. C. Hensley, L. W. Owen, R. M. DeVries, R. M. Gaedke, P. J. Riley, and S. T. Thornton, Phys. Rev. C **10**, 1429 (1974).
- ²⁹F. D. Becchetti, B. G. Harvey, D. G. Kovar, J. Mahoney, and M. S. Zisman, Phys. Rev. C **10**, 1846 (1974).
- ³⁰H. J. Körner, *Classical and Quantum Mechanical Aspects of Heavy Ion Collisions*, edited by H. L. Harney, P. Braun-Munzinger, and C. K. Gelbke (Springer-Verlag, Heidelberg, 1975), p. 39; J. D. Garrett, *ibid.*, p. 59; D. K. Scott, *ibid.*, p. 165; O. Hansen, *ibid.*, p. 295.
- ³¹W. Henning, Bull. Am. Phys. Soc. **20**, 621 (1975).
- ³²E. H. Auerbach, A. J. Baltz, P. D. Bond, C. Chasman, J. D. Garrett, K. W. Jones, S. Kahana, M. J. LeVine, M. Schneider, A. Z. Schwarzschild, and C. E. Thorn, Phys. Rev. Lett. **30**, 1078 (1973).
- ³³P. R. Christensen, O. Hansen, J. S. Larsen, D. Sinclair, and F. Videbaek, Phys. Lett. **45B**, 107 (1973).
- ³⁴M. F. Werby and W. Tobocman, Phys. Rev. C **10**, 1022 (1974).
- ³⁵M.-C. Lemaire, M. C. Mermaz, H. Sztark, and A. Cunsolo, Phys. Rev. **C10**, 1103 (1974).
- ³⁶M. J. LeVine, A. J. Baltz, P. D. Bond, J. D. Garrett, S. Kahana, and C. E. Thorn, Phys. Rev. C **10**, 1602 (1974); A. J. Baltz, P. D. Bond, J. D. Garrett, and S. Kahana, Phys. Rev. C (to be published).
- ³⁷M. S. Zisman, R. M. DeVries, J. G. Cramer, K.-L. Liu, Y.-D. Chan, and B. Cuengco, Phys. Rev. C **11**, 809 (1975).
- ³⁸W. Henning, D. G. Kovar, B. Zeidman, J. R. Erskine, and H. T. Fortune, Bull. Am. Phys. Soc. **19**, 504 (1974).

- ³⁹L. R. Greenwood, J. C. Stoltzfus, K. Katori, C. P. Cameron, and T. H. Braid, ANL Physics Division Informal Report No. PHY-1972B, May 1972 (unpublished).
- ⁴⁰B. Zeidman, W. Henning, and D. G. Kovar, Nucl. Instrum. Methods 118, 361 (1974).
- ⁴¹C. L. Fink, G. C. Morrison, and J. L. Yntema, in *Proceedings of the International Conference on Nuclear Physics, Munich, 1973*, edited by J. deBoer and H. J. Mang (North-Holland, Amsterdam/American Elsevier, New York, 1973), p. 460.
- ⁴²E. H. Auerbach, Brookhaven National Laboratory Report No. BNL-6562 (unpublished); modified by S. A. Zawadski, Argonne National Laboratory.
- ⁴³F. G. Perey, Optical-model code GENOA (unpublished).
- ⁴⁴U. C. Voos, W. von Oertzen, and R. Bock, Nucl. Phys. A135, 207 (1969); W. von Oertzen (unpublished).
- ⁴⁵M. C. Bertin, S. L. Tabor, B. A. Watson, Y. Eisen, and G. Goldring, Nucl. Phys. A167, 216 (1971).
- ⁴⁶K. O. Groeneveld, L. Meyer-Schützmeister, A. Richter, and U. Strohbusch, Phys. Rev. C 6, 805 (1972).
- ⁴⁷A. W. Obst, D. L. McShan, and R. H. Davis, Phys. Rev. C 6, 1814 (1972).
- ⁴⁸R. H. Siemssen, H. T. Fortune, R. Malmin, A. Richter, and J. W. Tippie, Phys. Rev. Lett. 25, 536 (1970).
- ⁴⁹A. M. Friedman, R. H. Siemssen, and J. G. Cuninghame, Phys. Rev. C 6, 2219 (1972).
- ⁵⁰Y. Eisen, R. A. Eisenstein, U. Smilansky, and Z. Vager, Nucl. Phys. A195, 513 (1972).
- ⁵¹J. S. Blair, in *Proceedings of the Fifth International Conference on Nuclear Reactions Induced by Heavy Ions, Heidelberg, 1969*, edited by R. Bock and W. R. Hering (North-Holland, Amsterdam, 1970), p. 1.
- ⁵²G. Igo, Phys. Rev. Lett. 1, 72 (1958).
- ⁵³R. M. DeVries, G. R. Satchler, and J. G. Cramer, Phys. Rev. Lett. 32, 1377 (1974).
- ⁵⁴A similar conclusion has recently been reached in the analysis of a single potential: P. J. Moffa, C. B. Dover, and J. P. Vary, Phys. Rev. C 13, 147 (1976); see also J. G. Cramer, M. S. Zisman, K. Liu, Y. Chan, B. Cuengco, and J. Wiborg, University of Washington, Nuclear Physics Laboratory, Annual Report, 1975 (unpublished), p. 128.
- ⁵⁵H. J. Körner, G. C. Morrison, L. R. Greenwood, and R. H. Siemssen, Phys. Rev. C 7, 107 (1973); A. Cunsolo, M. C. Lemaire, M. C. Mermaz, H. Sztark, K. L. Low, and T. Tamura, *ibid.* 10, 180 (1974).
- ⁵⁶J. R. Erskine, A. Marinov, and J. P. Schiffer, Phys. Rev. 142, 633 (1966).